Insights into human genetic variation and population history from 929 diverse genomes

Anders Bergstrom, Shane A. Mccarthy, Ruoyun Hui, Mohamed A. Almarri, Qasim Ayub, Petr Danecek, Yuan Chen, Sabine Felkel, Pille Hallast, Jack Kamm, et al.

Published in final edited form as:
Science. ; 367(6484): . doi:10.1126/science.aay5012.

Insights into human genetic variation and population history from 929 diverse genomes

Anders Bergström[1,2,*], **Shane A. McCarthy**[1,3,‡], **Ruoyun Hui**[3,4,‡], **Mohamed A. Almarri**[1,‡], **Qasim Ayub**[1,5,6], **Petr Danecek**[1], **Yuan Chen**[1], **Sabine Felkel**[1,7], **Pille Hallast**[1,8], **Jack Kamm**[1,3,9], **Hélène Blanché**[10,11], **Jean-François Deleuze**[10,11], **Howard Cann**[10,†], **Swapan Mallick**[12,13], **David Reich**[12,13], **Manjinder S. Sandhu**[1,14], **Pontus Skoglund**[2], **Aylwyn Scally**[3], **Yali Xue**[1,§], **Richard Durbin**[1,3,§], **Chris Tyler-Smith**[1,§,*]

[1]Wellcome Sanger Institute, Hinxton, CB10 1SA, UK

[2]The Francis Crick Institute, London, NW1 1AT, UK

[3]Department of Genetics, University of Cambridge, Cambridge, CB2 3EH, UK

[4]McDonald Institute for Archaeological Research, University of Cambridge, CB2 3ER, UK

[5]Monash University Malaysia Genomics Facility, Tropical Medicine and Biology Multidisciplinary Platform, 47500 Bandar Sunway, Malaysia

[6]School of Science, Monash University Malaysia, 47500 Bandar Sunway, Malaysia

[7]Institute of Animal Breeding and Genetics, University of Veterinary Medicine Vienna, Vienna, 1210, Austria

[8]Institute of Biomedicine and Translational Medicine, University of Tartu, Tartu 50411, Estonia

[9]Chan Zuckerberg Biohub, San Francisco, 94158, USA

[10]Centre d'Etude du Polymorphisme Humain, Fondation Jean Dausset, 75010 Paris, France

[11]GENMED Labex, Paris, France, ANR-10-LABX-0013

[12]Department of Genetics, Harvard Medical School, Boston, 02115, USA

[13]Broad Institute of Harvard and MIT, Cambridge, 02142, USA

[14]Department of Medicine, University of Cambridge, Cambridge, CB2 0QQ, UK

Abstract

Genome sequences from diverse human groups are needed to understand the structure of genetic variation in our species and the history of, and relationships between, different populations. We present 929 high-coverage genome sequences from 54 diverse human populations, 26 of which are physically phased using linked-read sequencing. Analyses of these genomes reveal an excess of previously undocumented common genetic variation private to each of southern Africa, central Africa, Oceania and the Americas, but an absence of such variants fixed between major geographical regions. We also find deep and gradual population separations within Africa, contrasting population size histories between hunter-gatherer and agriculturalist groups in the last 10,000 years, and a contrast between single Neanderthal but multiple Denisovan source populations contributing to present-day human populations.

Europe PMC Funders Author Manuscripts

Europe PMC Funders Author Manuscripts

One Sentence Summary—Genomes from 54 diverse populations expand the genomic record of human diversity and illuminate the history of our species

Structured Abstract

Introduction—Large-scale human genome sequencing studies to date have been limited to large, metropolitan populations or to small numbers of genomes from each group. Much remains to be understood about the extent and structure of genetic variation in our species and how it was shaped by past population separations, admixture, adaptation, size changes, and gene flow from archaic human groups. Larger numbers of genome sequences from more diverse populations are needed to illuminate these questions.

Rationale—We sequence 929 genomes from 54 geographically, linguistically and culturally diverse human populations to an average of 35x coverage, and analyze the variation among them. We also physically resolve the haplotype phase of 26 of these genomes using linked-read sequencing.

Results—We identify 67.3 million single-nucleotide polymorphisms (SNPs), 8.8 million small insertions or deletions (indels) and 40,736 copy number variants (CNVs). This includes hundreds of thousands of variants that had not been discovered by previous sequencing efforts but which are common in one or more population. We demonstrate benefits to the study of population relationships of genome sequences over ascertained array genotypes, particularly when involving African populations.

Populations in central and southern Africa, the Americas and Oceania each harbour tens to hundreds of thousands of private, common genetic variants. The majority of these variants arose as novel mutations rather than through archaic introgression, except in Oceanian populations where many private variants derive from Denisovan admixture. While some reach high frequencies, no variants are fixed between major geographical regions.

We estimate that the genetic separation between present-day human populations occurred mostly within the last 250,000 years. However, these early separations were gradual in nature and shaped by protracted gene flow. All populations thus still had some genetic contact more recently than this, but there is also evidence that a small fraction of present-day structure might be hundreds of thousands of years older. Most populations expanded in size over the last 10,000 years, but hunter-gatherer groups did not.

The low diversity among the Neanderthal haplotypes segregating in present-day populations indicates that, while more than one Neanderthal individual must have contributed genetic material to modern humans, there was likely only one major episode of admixture. In contrast, Denisovan haplotype diversity reflects a more complex history involving more than one episode of admixture.

We find small amounts of Neanderthal ancestry in West African genomes, most likely reflecting Eurasian admixture. Despite their very low levels or absence of archaic ancestry, African populations share many Neanderthal and Denisovan variants that are absent from Eurasia, reflecting how a larger proportion of the ancestral human variation has been maintained in Africa.

Conclusion—The discovery of substantial amounts of common genetic variation that was previously undocumented, and is geographically restricted, highlights the continued value of anthropologically informed study designs for understanding human diversity. The genome

sequences presented here are a freely available resource with relevance to population history, medical genetics, anthropology and linguistics.

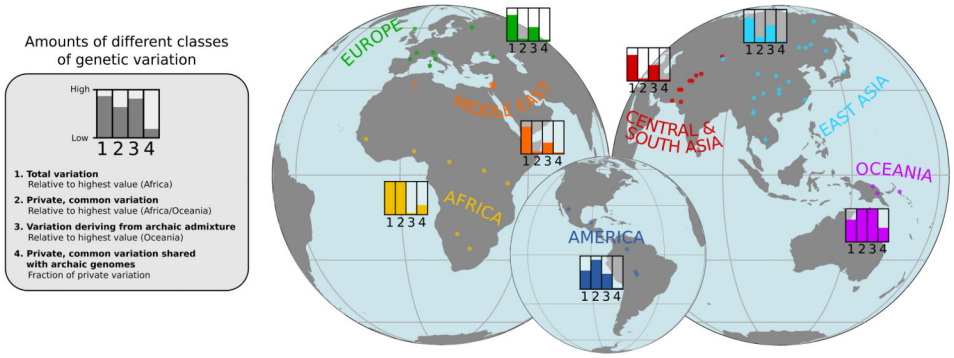

The structure of genetic variation across worldwide human populations.
A schematic illustration of the approximate amounts of four different classes of genetic variation found in different geographical regions. The origins of the populations included in the study are indicated by dots.

Genome sequences from diverse human groups can reveal the structure of genetic variation in our species and the history of, and relationships between, different populations. They also provide a framework for the design and interpretation of medical genetics studies. A consensus view of the history of our species includes divergence from the ancestors of the archaic Neanderthal and Denisovan groups 500,000-700,000 years ago, the appearance of anatomical modernity in Africa in the last few hundred thousand years, an expansion out of Africa and the Near East 50,000-70,000 years ago, with a reduction in genetic diversity in the descendant populations, admixture with archaic groups in Eurasia shortly after this and large-scale population growth, migration and admixture following multiple independent transitions from hunter-gatherer to food producing lifestyles in the last 10,000 years (1). However, much still remains to be understood about the extent to which population histories differed between continents and regions, and how this has shaped the present-day distribution and structure of genetic variation across the species. Large-scale genome sequencing efforts to date have been restricted to large, metropolitan populations and employed low-coverage sequencing (2), while those sampling human groups more widely have mostly been limited to 1-3 genomes per population (3, 4). The Human Genome Diversity Project (HGDP)-CEPH panel (5) has constituted a key resource to which several iterations of genetic assays have been applied (3, 6–12). Here, we present 929 high-coverage genome sequences from 54 geographically, linguistically and culturally diverse populations (Fig. 1A, table S1) from this panel, 142 of which were previously sequenced (3, 11, 13).

Genetic variant discovery across diverse human populations

We performed Illumina sequencing to an average coverage of 35x (min: 25x) and mapped reads to the GRCh38 reference assembly. We also used linked-read technology (14) to physically resolve the haplotype phase of 26 of these genomes from 13 populations (table S2). By analysing local sequencing coverage across the genome, we identified and excluded nine samples with large-scale alterations in chromosomal copy numbers that likely arose

during lymphoblastoid cell line culturing. The remaining individuals provided high-quality genotype calls (figs. S1, S2, S3). In this set of 929 genomes we identified 67.3 million single-nucleotide polymorphisms (SNPs), 8.8 million small insertions or deletions (indels) and 40,736 copy number variants (CNVs) (15). This is nearly as many as the 84.7 million SNPs discovered in 2504 individuals by the 1000 Genomes Project (2), reflecting increased sensitivity due to high-coverage sequencing as well as the greater diversity of human ancestries covered by the HGDP-CEPH panel. While the vast majority of the variants discovered by one of the studies but not the other are very low in frequency, the HGDP dataset contains substantial numbers of variants that were not identified by the 1000 Genomes Project but are common or even high-frequency in some populations: ~1 million variants at ≥20%, ~100,000 variants at ≥50% and even ~1000 variants fixed at 100% frequency in at least one sampled population (Fig. 1B). This highlights the importance of anthropologically informed sampling for uncovering human genetic diversity.

The unbiased variant discovery enabled by whole-genome sequencing avoids potential ascertainment biases associated with the pre-defined variant sets used on genotyping arrays. We find that while analyses of the SNPs included on commonly used arrays accurately recapitulate relationships between non-African populations, they sometimes dramatically distort relationships involving African populations (Fig. 1C). Some of the f_4-statistics commonly used to study population history and admixture (10) even shift sign when using array SNPs compared to when using all discovered SNPs, thus incorrectly reversing the direction of the implied ancestry relationship (for example: $f_4(BantuKenya,San;Mandenka,Sardinian)$ is positive (Z=2.9) using all variants but negative (Z=-3.11) when using commonly employed array sites). A set of 1.3 million SNPs ascertained as polymorphic among three archaic human genomes, mainly reflecting shared ancestral variation (69% of them being polymorphic in Africa), provide more accurate f_4-statistics than the variants on commonly used arrays, as well as more accurate F_{ST} values and cleaner estimates of individual ancestries in model-based clustering analyses (fig. S4), consistent with the theoretical properties of outgroup-ascertained variants (10).

Rare variants, largely absent from genotyping arrays, are more likely to derive from recent mutation and can therefore inform upon recently shared ancestry between individuals. The patterns of rare variant sharing across the 929 genomes reveal abundant structure (Fig. 2A), as well as a general pattern of greater between-population rare allele sharing among Eurasian as opposed to Oceanian and American populations. We do not find a general increase in the power to detect population relationships in the form of non-zero f_4-statistics when using all the discovered SNPs, most of which are rare, compared to using just the ~600,000 variants present on commonly used genotyping arrays (Fig. 1C). However, stratifying D-statistics by derived allele frequency can reveal more nuanced views of population relationships (16). In the presence of admixture, statistics of the form $D(Chimp,X;A,B)$, quantifying the extent to which the allele frequencies of X are closer to those of A or B, can take different values for variants that have different derived allele frequencies in X. For example, we find that the West African Yoruba have a closer relationship to non-Africans than to the central African Mbuti at high allele frequencies but the opposite relationship at low frequencies (Fig. 2B), suggesting recent gene flow between Mbuti and Yoruba since the divergence of non-Africans. An excess sharing of San with

Mandenka relative to Mbuti at low allele frequencies may similarly reflect low amounts of West African-related admixture into San (Fig. 2C) (17). The known Denisovan admixture in Oceanian populations manifests itself, without making use of any archaic genome sequences, in a greater affinity of African populations to Eurasians over Oceanians especially at variants that are fixed in Africans (Fig. 2D). In a manner analogous to this, at fixed variants the central African Biaka have much greater affinity to Yoruba than to the Mandenka, another West African population (Fig. 2E), which would be consistent with Mandenka having some ancestry that is basal to other African ancestries (18).

The Y chromosome sequences in the dataset recapitulate the well-understood structure of the human Y chromosome phylogeny, but also contain a number of rare lineages of interest (figs. S12, S13). An F* lineage representing the deepest known split in the FT branch that is carried by the vast majority of non-African men was found only once across the 1205 males of the 1000 Genomes Project (19). Here, we find it in five out of seven sampled males in the Lahu from Yunnan province in southern China (who also carry high levels of population-specific rare autosomal alleles (Fig. 2A)), pointing to the importance of East Asia for understanding the early dispersal of non-African Y chromosomes, and highlighting how sequencing of diverse human groups can recover genetic lineages that are globally rare.

The extremes of human genetic differentiation

We next studied the extremes of human genetic variation by identifying variants that are private to geographic regions (excluding individuals with likely recent admixture from other regions, table S4). We find no such private variants that are fixed in a given continent or major region (Fig. 3A-C). The highest frequencies are reached by a few tens of variants present at >70% (and a few thousands at >50%) in each of Africa, the Americas and Oceania. In contrast, the highest frequency variants private to either Europe, East Asia, the Middle East or Central and South Asia reach just 10-30%. This likely reflects greater genetic connectivity within Eurasia owing to culturally driven migrations and admixture in the last 10,000 years, events which did not involve the more isolated populations of the Americas and Oceania (1), allowing variation accumulating in the latter to remain private. Even comparing Central and South America, we find variants private to one region but absent from the other reaching >40% frequency. Within Africa, ~1000 variants private to the rainforest hunter-gatherer groups Mbuti and Biaka reach >30%, and the highly diverged San of southern Africa harbour ~100,000 private variants at >30% frequency, ~1000 at >60% and even about 20 that are fixed in our small sample of six individuals.

The vast majority of these geographically restricted variants reflect novel mutations that occurred after, or shortly before, the diversification of present-day groups, with >99% of alleles private to most non-African regions being the derived rather than the ancestral allele (Fig. 3D). Alleles private to Africa, however, include a higher proportion of ancestral alleles, and this proportion increases with allele frequency, reflecting old variants that have been lost outside of Africa. For the same reason, many high frequency private African variants are also found in available Neanderthal or Denisovan genomes (11, 16, 20) (Fig. 3E). The fraction of variants private to any given region outside of Africa that are shared with archaic genomes is very low, consistent with most or all gene flow from these archaic groups having

occurred before the diversification of present-day non-African ancestries. The exception to this is Oceania, in which at least ~35% of private variants present at ≥20% frequency are shared with the Denisovan genome. Generally, at least ~20% of common (>10% allele frequency) variants that are present outside of Africa but absent inside Africa are shared with and thus likely derive from admixture with Neanderthals and Denisovans (Fig. 3F). The remaining up to ~80% of such common variants are more likely to have derived from novel mutations, which thus have been a stronger force than archaic admixture in introducing novel variants into present-day human populations.

Indel variants private to geographic regions display frequency distributions similar to those of SNPs, although reduced in overall numbers by approximately 10-fold (Fig. 3B). The same is mostly true of CNVs, with an even greater reduction in overall numbers, except for a slight excess of high-frequency private CNVs in Oceanians over what would be expected on the basis of the number of private Oceanian SNPs (Fig. 3C, fig. S5). Several of these variants are shared with the available Denisovan genome, suggesting that, relative to other variant classes and geographical regions, positive selection may have acted with a disproportionate strength on copy number variants of archaic origin in the history of Oceanian populations.

Effective population size histories

We next examined what present-day patterns of genetic variation can tell us about the past demographic histories of different human populations. The distribution of coalescence times between chromosomes sampled from the same population can be used to infer changes in effective population size over time (21, 22). However, resolution in recent times is limited when analysing single human genomes, and haplotype phasing errors can cause artefacts when using multiple genomes (23, 24). We therefore applied SMC++ (24) which extends this approach to incorporate information from the site frequency spectrum as estimated from a larger number of unphased genomes, enabling inference of effective population sizes into more recent time periods (Fig. 4A). In Europe and East Asia, most populations are inferred to have experienced major growth in the last 10,000 years, but less so in more isolated groups, including the European Sardinians, Basques, Orkney islanders, the southern Chinese Lahu and the Siberian Yakut. In Africa, while the sizes of agriculturalist populations increased over the last 10,000 years, those of the hunter-gatherer groups, Biaka, Mbuti and San, saw no growth or even declined. These findings may reflect a more general pattern of human prehistory, in which hunter-gatherer groups which previously might have been more numerous and widespread decreased in size as agriculturalist groups expanded (25).

We also find tentative evidence for population growth in the ancestors of Native Americans coinciding with entry into the American continents ~15 kya (Fig. 4B), mirroring observations of rapid diversification of mitochondrial and Y-chromosome lineages at this time (26, 27) but not previously observed with autosomal data. The inference is sensitive to SMC++ parameter settings and likely counteracted by very recent bottlenecks in the Native American groups, but other populations do not display similar histories under these parameter settings (fig. S10). While this finding might be a technical artefact and will require further validation, the inferred growth rate exceeds even those of large European and

Europe PMC Funders Author Manuscripts

East Asian populations in the last 10,000 years, suggesting this could be one of the most dramatic growth episodes in modern human population history.

While informative, these analyses still appear to have limited resolution to infer more fine-scale population size histories during the transitions to agriculture, metal ages and other cultural processes that have occurred during the last 10,000 years. This might require yet larger sample sizes, novel analytical methods that exploit other features of genetic variation (28), or both.

The time depth and mode of human population separations

We used the 26 genomes physically phased by linked-read technology to study the time-course of population separations using the MSMC2 method (22, 29). As a heuristic approximation to the split time between two populations we take the point at which the estimated rate of coalescence between them is half of the rate of coalescence within them, but we also assess how gradual or extended over time the splits were by comparing the shape of the curves to those obtained by running the method on simulated instant split scenarios without subsequent gene flow. Assuming a mutation rate of 1.25×10^{-8} per base-pair per generation (30) and a generation time of 29 years (31), our midpoint estimates suggest (Fig. 5A) splits between the two central African rain forest hunter-gatherer groups Mbuti and Biaka ~62 kya, Mbuti and the West African Yoruba ~69 kya, Yoruba and the southern African San ~126 kya and between San and both of Biaka and Mbuti ~110 kya. Non-Africans have separation midpoints from Yoruba ~76 kya, Biaka ~96 kya, Mbuti ~123 kya and, representing the deepest split in the dataset, from San ~162 kya. However, all of these curves are clearly inconsistent with clean splits, suggesting a picture where genetic separations within Africa were gradual and shaped by ongoing gene flow over tens of thousands of years. For example, there is evidence of gene flow between San and Biaka until at least 50 kya, and between each of Mbuti, Biaka and Yoruba until the present day or as recently as the method can infer.

For the deepest splits, there is some evidence of genetic separation dating back to before 300 or even 500 kya, in the sense that even by that time the rate of coalescence between populations still differs from that within populations. The implication of this would be that there lived populations already at this time which have contributed more to some present-day human ancestries than to others. We find that a small degree of such deep structure in MSMC2 curves might be spuriously caused by batch effects associated with sequencing and genotyping pairs of chromosomes from diploid human samples together, but that such effects are not large enough to fully explain the differences in coalescence rates at these time scales (fig. S7). However, even if this signal reflects actual ancient population structure, its magnitude is such that it would only apply to small fractions of present-day ancestries. An analogy to this is how Neanderthal and Denisovan admixture results in a few percent of non-African ancestries separating from some African ancestries approximately half a million years ago, while most of the ancestry was connected until much more recently. We argue, in the light of such composite ancestries in present-day human populations and the clear deviation of our MSMC2 results from instant split behaviours, that single point estimates are inadequate for describing the timing of early modern human population separations. A more

meaningful summary of our results might be that the structure we observe among human populations today formed predominantly during the last 250 ky, with continued genetic contact between all populations during much of this time, but also a small fraction of present-day ancestries retaining traces of structure that is older than this, potentially by hundreds of thousands of years.

We also applied MSMC2 to the history of separation between archaic and modern human populations. While the method relies on phased haplotypes, the high degree of homozygosity of Neanderthals and Denisovans means that it might still perform well despite the absence of phase information for heterozygous sites in these genomes. The midpoint estimates suggest that modern and archaic populations separated 550-700 kya (Fig. 5A), in line with, but potentially slightly earlier than, estimates obtained with other methods (16, 20). These results also provide relative constraints on the overall time depth of modern human structure that are independent of the mutation rate we use to scale the results, in the sense that the deepest modern human midpoints are less than one-third of the age of the midpoints of the archaic curves. However, the deep tails of some modern human curves partly overlap a time period when genetic separation from the archaics might still not have been complete. The separation between archaic and modern humans appears more sudden than those between different modern human populations, and only slightly less sudden than expected under an instant split scenario, suggesting a qualitatively different mode of separation between modern and archaic groups than between modern human groups within Africa. While the divergence time between modern human and Neanderthal mitochondrial genomes shows that there is at least some ancestry shared more recently than 500 kya (32), these MSMC2 results suggest that post-split gene flow to and from the archaic groups, likely geographically restricted to Eurasia, overall would have been limited.

Outside of Africa, the time depths of population splits are in line with previous estimates (3, 4, 22), with all populations sharing most of their ancestry within the last 70 kya (Fig. 5B). Our analyses of these physically phased genomes do not replicate a previously observed earlier divergence of West Africans from Oceanians than from Eurasians in MSMC analyses (4, 29), suggesting those results were caused by some artefact of statistical phasing. Instead, all non-African populations display very similar histories of separation from African populations (fig. S6). Like those within Africa, many curves between non-African populations are more gradual than instant split simulations. However, some curves, including those between the Central American Pima and the South American Karitiana, between Han Chinese and the Siberian Yakut, or between the European Sardinians and the Near Eastern Druze, do not deviate appreciably from those expected under instant splits. This suggests that once modern humans had expanded into the geographically diverse and fragmented continents outside of Africa, populations would sometimes separate suddenly and without much subsequent gene flow.

We also fit simple pairwise split models for the complete set of 1431 population pairs to the site-frequency spectrum using momi2 (33), obtaining estimates with high concordance to the MSMC2 midpoints ($r = 0.93$). This much larger set of split time estimates is consistent with present-day populations sharing the majority of their ancestry within the last 200 kya. Using these estimates, we also find that the strength of allele frequency differentiation between

populations (F_{ST}) relative to split times is about three times greater outside than inside of Africa (Fig. 5C). This could partly reflect increased rates of drift in some non-African populations, but is likely largely explained by the amplifying effects on F_{ST} of the reduced diversity of these groups following their shared bottleneck event (34).

The genetic contribution of archaic hominins to present-day human populations

We estimate an average of 2.4% and 2.1% Neanderthal ancestry in eastern non-Africans and western non-Africans, respectively. We estimate 2.8% (95% confidence interval: 2.1-3.6%) Denisovan ancestry in Papuan highlanders (15), substantially lower than the first estimate of 4-6% (35) based on less comprehensive modern and archaic data, but only slightly lower than more recent estimates (11, 36, 37). The proportion of ancestry that remains in present-day Oceanian populations after the Denisovan admixture is thus likely not much higher than the amount of Neanderthal ancestry that remains in non-Africans generally.

We identified Neanderthal and Denisovan segments in non-African genomes using a hidden Markov model (15), and studied the diversity of these haplotypes to learn about the structure of these admixture events and whether they involved one or more source populations. For Neanderthals, several lines of evidence are consistent with there having been a single source with no apparent contribution from any additional population which was detectably different in terms of ancestry, geographical distribution or admixture time. Neanderthal segments recovered from modern genomes across the world show very similar distributions along the genome (fig. S18 and table S8) and profiles of divergence to available archaic genomes (fig. S19), and different Neanderthal haplotypes detected at the same location in modern genomes rarely form geographically structured clusters (fig. S23, table S10). The structure of absolute divergence (D_{XY}) in Neanderthal segments between pairs of non-African populations mirrors that in unadmixed segments (Fig. 6A), suggesting a shared admixture event before these populations diverged from each other. A substantial later episode of admixture from Neanderthals into one or more modern populations would have resulted in greater structure (more divergence between some populations) in the Neanderthal segments relative to that in unadmixed segments. Instead, the diversity in unadmixed segments relative to that in Neanderthal segments is higher in western than in eastern non-Africans, perhaps due to gene flow from a source with little or no Neanderthal ancestry into the former (38). Although phylogenetic reconstructions indicate that some regions in the genome contain more than 10 different introgressing Neanderthal haplotypes (Fig. 6B, table S9), thus clearly ruling out the scenario of a single contributing Neanderthal individual, the average genetic diversity of admixed Neanderthal sequences is limited (Fig. 6B,C). Coalescent simulations suggest that, genome-wide, as few as 2-4 founding haplotypes are sufficient to produce the observed distribution of haplotype network sizes.

In contrast, Denisovan segments show evidence of a more complex admixture history. Segments in Oceania are distinct from those in East Asia, the Americas and South Asia, as shown by their different distribution along the genome (fig. S18 and table S8), high D_{XY} values (Fig. 6A) and a clear separation in most haplotype networks between these two

geographical groups (fig. S24, table S10), corresponding to a deep divergence between the Denisovan source populations. East Asian populations also harbour some Denisovan segments that are very similar to the Altai Denisovan genome but which are absent from Oceania (fig. S19). This is consistent with the Denisovan ancestry in Oceania having originated from a separate gene flow event not experienced in other parts of the world (39). We do not, however, find clear evidence of more than one source in Oceanians (40). The more complicated structure of the Denisovan segments in East Asia (and likely also in the Americas and South Asia) is difficult to explain by one or even two admixture events, and may possibly reflect encounters with multiple Denisovan populations by the ancestors of modern humans in Asia. Some Denisovan haplotypes found in Cambodians are somewhat distinct from those in the rest of East Asia with tentative connections to those in Oceania. Overall, these results paint a picture of an admixture history from Denisovan-related populations into modern humans that is substantially more complex than the history of admixture from Neanderthals.

In MSMC2 analyses, we find that non-Africans display clear modes of non-zero cross-coalescence rates with the Vindija Neanderthal in recent time periods (<100 kya), providing an additional line of evidence for the known admixture episode without requiring assumptions about African populations lacking admixture (Fig. 6D, fig. S8). The Denisovan gene flow into Oceanians is also visible in these analyses but is less pronounced and substantially shifted backwards in time (fig. S8), consistent with the introgressing population being highly diverged from the sequenced individual from the Altai mountains. The West African Yoruba also display a Neanderthal admixture signal, similar in shape but much less pronounced than the signal in non-Africans (Fig. 6D, fig S9). Other African populations do not clearly display the same behaviour. These results provide evidence for low amounts of Neanderthal ancestry in West Africa, consistent with previous results based on other approaches (16, 20), and we estimate this at 0.18%±0.06% in Yoruba using an f_4-ratio (assuming Mbuti has none). The most likely source for this is West Eurasian admixture (41), and assuming a simple linear relationship to Neanderthal ancestry, our estimate implies 8.6%±3% Eurasian ancestry in Yoruba.

While there is an excess of haplotypes deriving from archaic admixture in non-Africans, many single variants present in archaic populations are also present in Africans due to their having segregated in the population ancestral to archaic and modern humans, and some of these variants were subsequently lost in non-Africans due to increased genetic drift. Counting how many of the variants carried in heterozygote state in archaic individuals are segregating in balanced sets of African and non-African genomes, we find that more Vindija Neanderthal variants survive in non-Africans than in Africans (31.0% vs 26.4%). However, more Denisovan variants survive in Africans (18.9% vs 20.3%). These numbers might change if larger numbers of Oceanian populations were surveyed, but they highlight how the high levels of genetic diversity in African populations mean that, despite having received much less or no Neanderthal and Denisovan admixture, they still retain a substantial, and only partly overlapping (Fig. 3E), subset of the variants which were segregating in late archaic populations.

Discussion

While the number of human genomes sequenced as part of medically motivated genetic studies is rapidly growing into the hundreds of thousands, the number resulting from anthropologically informed sampling to characterize human diversity still remains in the hundreds to low thousands. With the set of 929 genomes from 54 diverse human populations presented here, we greatly extend the number of high-coverage genomes freely available to the research community as part of human global diversity datasets, and substantially expand the catalogue of genetic variation to many underrepresented ancestries. Our analyses of these genomes highlight several aspects of human genetic diversity and history, including the extent and source of geographically restricted variants in different parts of the world, the time depth of separation and extensive gene flow between populations in Africa, a potentially dramatic population expansion following entry into the Americas and a simple pattern of Neanderthal admixture contrasting with a more complex pattern of Denisovan admixture.

One aim of the 1000 Genomes Project (2) was to capture most common human genetic variation, which it achieved in the populations included in the study. However, the more diverse HGDP dataset reveals that there are several human ancestries for which this aim was not achieved, and which harbour substantial amounts of genetic variation, some of it common, that so far has been documented poorly or not at all. This is particularly true of Africa and the ancestries represented by the southern African San, and central African Mbuti and Biaka groups. Outside of Africa, Oceanian populations represent one of the major lineages of non-African ancestries and have substantial amounts of private variation, some of it deriving from Denisovan admixture. Any biomedical implications of variants common in these populations but rare or absent elsewhere are unknown, and will remain unknown until genetic association studies are extended to include these and other currently underrepresented ancestries.

Our analyses demonstrate the value of generating multiple high-coverage whole-genome sequences to characterise variation in a population, compared to genotyping using arrays, sequencing to low-coverage or sequencing just small numbers of genomes. In particular, such an approach enables unbiased variant discovery, including of large numbers of low-frequency variants, and higher resolution assessments of allele frequencies. The experimental phasing of haplotypes using linked-read technology aids analyses of deep human population history and structural variation, and is now becoming a feasible alternative to statistical phasing, especially useful in diverse populations. However, short read sequencing still imposes limitations on the ability to identify more complex structural variation. We expect the application of long-read or linked-read sequencing technologies to large sets of diverse human genomes, combined with de-novo assembly or variation graph (42) approaches that are less reliant on the human reference assembly, to unveil these additional layers of human genetic diversity.

While the HGDP genome dataset substantially expands our genomic record of human diversity, it too contains considerable gaps in its geographical, linguistic and cultural coverage. We therefore argue for the importance of continued sequencing of diverse human

genomes. Given the scale of ongoing medical and national genome projects, producing high-coverage genome sequences for at least ten individuals from each of the approximately 7000 (43) human linguistic groups would now arguably not be an overly ambitious goal for the human genomics community. Such an achievement would represent a scientifically and culturally important step towards diversity and inclusion in human genomics research.

Materials and methods summary

We sequenced DNA, extracted from the lymphoblastoid cell lines of the HGDP-CEPH panel (5), on Illumina HiSeq X machines, and incorporated data from a subset of samples that had been previously sequenced (3, 11). Reads were mapped to the GRCh38 human reference assembly. We applied per-sample caps on the mapping quality of reads to counteract the effects of low-level index hopping in multiplexed sequencing runs. We analyzed patterns of sequencing coverage along the chromosomes to identify any large-scale copy number deviations that arose during cell line culturing, and excluded nine samples with such deviations, leaving 929 samples.

Genotypes were called using GATK HaplotypeCaller (44) v3.5.0 and filtered by setting to missing any genotype with a GQ (Genotype Quality) or RGQ (Reference Genotype Quality) value equal to or lower than 20, or a DP (depth) value equal to or greater than 1.65 times the genome-wide average coverage for the given sample. We also flagged sites displaying excess heterozygosity and excluded these from analyses. We constructed a genome accessibility mask largely based on the 1000 Genomes Project (2) “strict mask” and restricted analyses to these regions. Batch effects between library types observed when analysing unfiltered genotypes were not observed after applying the genotype filters and restricting to the mask, but we cannot rule out that more subtle effects persist. We reassessed the population labels used in the previous literature on the HGDP-CEPH panel to arrive at 54 labels which we use in analyses, along with the seven regional/continental labels previously used (6). We constructed 10x Genomics linked-read libraries (14) and sequenced these on Illumina HiSeq X machines for 26 of the individuals, from 13 globally representative populations, to physically resolve their haplotype phase and aid analyses of structural variation.

We used ADMIXTOOLS (10) v5.0 to compute f_4 and D-statistics and EIGENSOFT (45) v6.0.1 to compute F_{ST} statistics. To identify variants that are private to geographical regions while avoiding the effects of recent admixture between regions, we used the model-based clustering program ADMIXTURE (46) to determine which individuals to use as the ingroup and outgroup for each region.

We used MSMC2 (22, 29) to study the time depth and nature of population separations, using the 13 populations for which we had physically phased genomes for two individuals each. By site-frequency spectrum modelling using momi2 (33) we also estimated all possible pairwise population divergence times under simple, clean split scenarios. We used SMC++ (24) to infer effective population size histories, using all available genomes for a given population. For all demographic analyses, we scaled results using a mutation rate of 1.25×10-8 per site per generation (30) and a generation time of 29 years (31).

Europe PMC Funders Author Manuscripts

Europe PMC Funders Author Manuscripts

To identify segments in modern human genomes deriving from archaic admixture, we used a Hidden Markov Model trained on simulated haplotypes. The model decodes haplotypes into archaic or unadmixed on the basis of the allele sharing patterns between sub-Saharan Africans, one or more archaic genomes, and the given genome under examination. We analysed the properties of the inferred haplotypes, including their nucleotide diversity, spatial distributions along the genome and phylogenetic relationships and ages as inferred using haplotype networks.

Detailed descriptions of materials and methods are available in the supplementary materials.

Supplementary Material

Refer to Web version on PubMed Central for supplementary material.

Footnotes

*Correspondence to. ab34@sanger.ac.uk (A.B.); cts@sanger.ac.uk (C.T.-S.)

‡These authors contributed equally to this work.

§These authors contributed equally to this work.

†Deceased.

Data and materials availability: Raw read alignments are available from the European Nucleotide Archive under study accession PRJEB6463. Processed per-sample read alignment files are made available by the International Genome Sample Resource at the European Bioinformatics Institute (EMBL-EBI) (http://ftp.1000genomes.ebi.ac.uk/vol1/ftp/data_collections/HGDP/). The 10x Genomics sequencing data generated for 26 samples are available at the European Nucleotide Archive under study accession PRJEB14173. Genotype calls and other downstream analysis files are available from the Wellcome Sanger Institute (ftp://ngs.sanger.ac.uk/production/hgdp). DNA extracts from the samples in the HGDP-CEPH collection can be obtained from the CEPH Biobank at Fondation Jean Dausset-CEPH in Paris, France (http://www.cephb.fr/en/hgdp_panel.php).

Acknowledgments

We thank the sample donors who made this research possible, as well as the CEPH Biobank, Paris, France (BIORESOURCES) at Fondation Jean Dausset-CEPH, for maintaining the cell line resource and distributing DNA. We thank the Wellcome Sanger Institute sequencing facility for generating data, and Susan Fairley and colleagues at the International Genome Sample Resource for incorporating and hosting data. We thank J. Terhorst, S. Schiffels, R. Handsaker, D. Gurdasani and members of the Tyler-Smith and Durbin groups for useful advice and discussions.

Funding

A.B., S.A.M., M.A.A, Q.A., P.D., Y.C., S.F., P.H., J.K, M.S.S., Y.X., R.D. and C.T.-S. were supported by Wellcome grants 098051 and 206194, and S.A.M. and R.D. also by Wellcome grant 207492. A.B. and P.S. were supported by the Francis Crick Institute (FC001595) which receives its core funding from Cancer Research UK, the UK Medical Research Council and the Wellcome Trust. P.S. was also supported by the European Research Council (grant no. 852558) and the Wellcome Trust (217223/Z/19/Z). R.H. was supported by a Gates Cambridge scholarship. P.H. was supported by Estonian Research Council Grant PUT1036. D.R. is an Investigator of the Howard Hughes Medical Institute.

Europe PMC Funders Author Manuscripts

References

1. Nielsen R, et al. Tracing the peopling of the world through genomics. Nature. 2017; 541:302–310. [PubMed: 28102248]
2. 1000 Genomes Project Consortium. A global reference for human genetic variation. Nature. 2015; 526:68–74. [PubMed: 26432245]
3. Mallick S, et al. The Simons Genome Diversity Project: 300 genomes from 142 diverse populations. Nature. 2016; 538:201–206. [PubMed: 27654912]
4. Pagani L, et al. Genomic analyses inform on migration events during the peopling of Eurasia. Nature. 2016; 538:238–242. [PubMed: 27654910]
5. Cann HM, et al. A human genome diversity cell line panel. Science. 2002; 296:261–262. [PubMed: 11954565]
6. Rosenberg NA, et al. Genetic structure of human populations. Science. 2002; 298:2381–2385. [PubMed: 12493913]
7. Jakobsson M, et al. Genotype, haplotype and copy-number variation in worldwide human populations. Nature. 2008; 451:998–1003. [PubMed: 18288195]
8. Li JZ, et al. Worldwide human relationships inferred from genome-wide patterns of variation. Science. 2008; 319:1100–1104. [PubMed: 18292342]
9. Shi W, et al. A worldwide survey of human male demographic history based on Y-SNP and Y-STR data from the HGDP-CEPH populations. Mol Biol Evol. 2010; 27:385–393. [PubMed: 19822636]
10. Patterson N, et al. Ancient admixture in human history. Genetics. 2012; 192:1065–1093. [PubMed: 22960212]
11. Meyer M, et al. A high-coverage genome sequence from an archaic Denisovan individual. Science. 2012; 338:222–226. [PubMed: 22936568]
12. Lippold S, et al. Human paternal and maternal demographic histories: insights from high-resolution Y chromosome and mtDNA sequences. Investig Genet. 2014; 5:13.
13. Raghavan M, et al. Genomic evidence for the Pleistocene and recent population history of Native Americans. Science. 2015; 349
14. Zheng GX, et al. Haplotyping germline and cancer genomes with high-throughput linked-read sequencing. Nat Biotechnol. 2016; 34:303–311. [PubMed: 26829319]
15. Materials and methods are available as supplementary materials.
16. Prufer K, et al. The complete genome sequence of a Neanderthal from the Altai Mountains. Nature. 2014; 505:43–49. [PubMed: 24352235]
17. Pickrell JK, et al. Ancient west Eurasian ancestry in southern and eastern Africa. Proc Natl Acad Sci U S A. 2014; 111:2632–2637. [PubMed: 24550290]
18. Skoglund P, et al. Reconstructing Prehistoric African Population Structure. Cell. 2017; 171:59–71. [PubMed: 28938123]
19. Poznik GD, et al. Punctuated bursts in human male demography inferred from 1,244 worldwide Y-chromosome sequences. Nat Genet. 2016; 48:593–599. [PubMed: 27111036]
20. Prufer K, et al. A high-coverage Neandertal genome from Vindija Cave in Croatia. Science. 2017; 358:655–658. [PubMed: 28982794]
21. Li H, Durbin R. Inference of human population history from individual whole-genome sequences. Nature. 2011; 475:493–496. [PubMed: 21753753]
22. Schiffels S, Durbin R. Inferring human population size and separation history from multiple genome sequences. Nat Genet. 2014; 46:919–925. [PubMed: 24952747]
23. Song S, Sliwerska E, Emery S, Kidd JM. Modeling Human Population Separation History Using Physically Phased Genomes. Genetics. 2017; 205:385–395. [PubMed: 28049708]
24. Terhorst J, Kamm JA, Song YS. Robust and scalable inference of population history from hundreds of unphased whole genomes. Nat Genet. 2017; 49:303–309. [PubMed: 28024154]
25. Excoffier L, Schneider S. Why hunter-gatherer populations do not show signs of pleistocene demographic expansions. Proc Natl Acad Sci U S A. 1999; 96:10597–10602. [PubMed: 10485871]

26. Llamas B, et al. Ancient mitochondrial DNA provides high-resolution time scale of the peopling of the Americas. Sci Adv. 2016; 2:e1501385. [PubMed: 27051878]
27. Pinotti T, et al. Y Chromosome Sequences Reveal a Short Beringian Standstill, Rapid Expansion, and early Population structure of Native American Founders. Curr Biol. 2019; 29:149–157. [PubMed: 30581024]
28. Browning SR, Browning BL. Accurate Non-parametric Estimation of Recent Effective Population Size from Segments of Identity by Descent. Am J Hum Genet. 2015; 97:404–418. [PubMed: 26299365]
29. Malaspinas AS, et al. A genomic history of Aboriginal Australia. Nature. 2016; 538:207–214. [PubMed: 27654914]
30. Scally A. The mutation rate in human evolution and demographic inference. Curr Opin Genet Dev. 2016; 41:36–43. [PubMed: 27589081]
31. Fenner JN. Cross-cultural estimation of the human generation interval for use in genetics-based population divergence studies. Am J Phys Anthropol. 2005; 128:415–423. [PubMed: 15795887]
32. Posth C, et al. Deeply divergent archaic mitochondrial genome provides lower time boundary for African gene flow into Neanderthals. Nat Commun. 2017; 8
33. Kamm J, Terhorst J, Durbin R, Song YS. Efficiently Inferring the Demographic History of Many Populations With Allele Count Data. Journal of the American Statistical Association. 2019; 0:1–16.
34. Jakobsson M, Edge MD, Rosenberg NA. The relationship between F(ST) and the frequency of the most frequent allele. Genetics. 2013; 193:515–528. [PubMed: 23172852]
35. Reich D, et al. Genetic history of an archaic hominin group from Denisova Cave in Siberia. Nature. 2010; 468:1053–1060. [PubMed: 21179161]
36. Qin P, Stoneking M. Denisovan Ancestry in East Eurasian and Native American Populations. Mol Biol Evol. 2015; 32:2665–2674. [PubMed: 26104010]
37. Vernot B, et al. Excavating Neandertal and Denisovan DNA from the genomes of Melanesian individuals. Science. 2016; 352:235–239. [PubMed: 26989198]
38. Lazaridis I, et al. Genomic insights into the origin of farming in the ancient Near East. Nature. 2016; 536:419–424. [PubMed: 27459054]
39. Browning SR, Browning BL, Zhou Y, Tucci S, Akey JM. Analysis of Human Sequence Data Reveals Two Pulses of Archaic Denisovan Admixture. Cell. 2018; 173:53–61. [PubMed: 29551270]
40. Jacobs GS, et al. Multiple Deeply Divergent Denisovan Ancestries in Papuans. Cell. 2019; 177:1010–1021. [PubMed: 30981557]
41. Lazaridis I, et al. Paleolithic DNA from the Caucasus reveals core of West Eurasian ancestry. bioRxiv 423079. 2018
42. Garrison E, et al. Variation graph toolkit improves read mapping by representing genetic variation in the reference. Nat Biotechnol. 2018; 36:875–879. [PubMed: 30125266]
43. Simons GF, Fennig CD. Ethnologue: Languages of the World (Twenty-first edition). 2018
44. McKenna A, et al. The Genome Analysis Toolkit: a MapReduce framework for analyzing next-generation DNA sequencing data. Genome Res. 2010; 20:1297–1303. [PubMed: 20644199]
45. Patterson N, Price AL, Reich D. Population structure and eigenanalysis. PLoS Genet. 2006; 2:e190. [PubMed: 17194218]
46. Alexander DH, Novembre J, Lange K. Fast model-based estimation of ancestry in unrelated individuals. Genome Res. 2009; 19:1655–1664. [PubMed: 19648217]
47. Li H, Durbin R. Fast and accurate short read alignment with Burrows-Wheeler transform. Bioinformatics. 2009; 25:1754–1760. [PubMed: 19451168]
48. Tischler G, Leonard S. biobambam: tools for read pair collation based algorithms on BAM files. Source Code Biol Med. 2014
49. Sherry ST, et al. dbSNP: the NCBI database of genetic variation. Nucleic Acids Res. 2001; 29:308–311. [PubMed: 11125122]
50. Jun G, et al. Detecting and estimating contamination of human DNA samples in sequencing and array-based genotype data. Am J Hum Genet. 2012; 91:839–848. [PubMed: 23103226]

51. Li H. A statistical framework for SNP calling, mutation discovery, association mapping and population genetical parameter estimation from sequencing data. Bioinformatics. 2011; 27:2987–2993. [PubMed: 21903627]
52. Bergström A, et al. A Neolithic expansion, but strong genetic structure, in the independent history of New Guinea. Science. 2017; 357:1160–1163. [PubMed: 28912245]
53. Handsaker RE, et al. Large multiallelic copy number variations in humans. Nat Genet. 2015; 47:296–303. [PubMed: 25621458]
54. Neph S, et al. BEDOPS: high-performance genomic feature operations. Bioinformatics. 2012; 28:1919–1920. [PubMed: 22576172]
55. Delaneau O, Marchini J, C. Genomes Project, C. Genomes Project. Integrating sequence and array data to create an improved 1000 Genomes Project haplotype reference panel. Nat Commun. 2014; 5
56. Loh PR, Palamara PF, Price AL. Fast and accurate long-range phasing in a UK Biobank cohort. Nat Genet. 2016; 48:811–816. [PubMed: 27270109]
57. Browning BL, Browning SR. Genotype Imputation with Millions of Reference Samples. Am J Hum Genet. 2016; 98:116–126. [PubMed: 26748515]
58. Rosenberg NA, et al. Clines, clusters, and the effect of study design on the inference of human population structure. PLoS Genet. 2005; 1:e70. [PubMed: 16355252]
59. Staab PR, Zhu S, Metzler D, Lunter G. scrm: efficiently simulating long sequences using the approximated coalescent with recombination. Bioinformatics. 2015; 31:1680–1682. [PubMed: 25596205]
60. Poznik GD, et al. Sequencing Y chromosomes resolves discrepancy in time to common ancestor of males versus females. Science. 2013; 341:562–565. [PubMed: 23908239]
61. Quinlan AR, Hall IM. BEDTools: a flexible suite of utilities for comparing genomic features. Bioinformatics. 2010; 26:841–842. [PubMed: 20110278]
62. Stamatakis A. RAxML version 8: a tool for phylogenetic analysis and post-analysis of large phylogenies. Bioinformatics. 2014; 30:1312–1313. [PubMed: 24451623]
63. Drummond AJ, Rambaut A, Shapiro B, Pybus OG. Bayesian coalescent inference of past population dynamics from molecular sequences. Mol Biol Evol. 2005; 22:1185–1192. [PubMed: 15703244]
64. Drummond AJ, Rambaut A. BEAST: Bayesian evolutionary analysis by sampling trees. BMC Evol Biol. 2007; 7:214. [PubMed: 17996036]
65. Fu Q, et al. Genome sequence of a 45,000-year-old modern human from western Siberia. Nature. 2014; 514:445–449. [PubMed: 25341783]
66. Zhao H, et al. CrossMap: a versatile tool for coordinate conversion between genome assemblies. Bioinformatics. 2014; 30:1006–1007. [PubMed: 24351709]
67. Skoglund P, et al. Genetic evidence for two founding populations of the Americas. Nature. 2015; 525:104–108. [PubMed: 26196601]
68. Haak W, et al. Massive migration from the steppe was a source for Indo-European languages in Europe. Nature. 2015; 522:207–211. [PubMed: 25731166]
69. Reich D, et al. Denisova admixture and the first modern human dispersals into Southeast Asia and Oceania. Am J Hum Genet. 2011; 89:516–528. [PubMed: 21944045]
70. Kelleher J, Etheridge AM, McVean G. Efficient Coalescent Simulation and Genealogical Analysis for Large Sample Sizes. PLoS Comput Biol. 2016; 12:e1004842. [PubMed: 27145223]
71. Vernot B, Akey JM. Resurrecting surviving Neandertal lineages from modern human genomes. Science. 2014; 343:1017–1021. [PubMed: 24476670]
72. Sankararaman S, et al. The genomic landscape of Neanderthal ancestry in present-day humans. Nature. 2014; 507:354–357. [PubMed: 24476815]
73. Li H. Toward better understanding of artifacts in variant calling from high-coverage samples. Bioinformatics. 2014; 30:2843–2851. [PubMed: 24974202]
74. Nei M, Li WH. Mathematical model for studying genetic variation in terms of restriction endonucleases. Proc Natl Acad Sci U S A. 1979; 76:5269–5273. [PubMed: 291943]

75. Lazaridis I, et al. Ancient human genomes suggest three ancestral populations for present-day Europeans. Nature. 2014; 513:409–413. [PubMed: 25230663]

76. Paradis E. pegas: an R package for population genetics with an integrated-modular approach. Bioinformatics. 2010; 26:419–420. [PubMed: 20080509]

77. Saillard J, Forster P, Lynnerup N, Bandelt HJ, Norby S. mtDNA variation among Greenland Eskimos: the edge of the Beringian expansion. Am J Hum Genet. 2000; 67:718–726. [PubMed: 10924403]

Europe PMC Funders Author Manuscripts

Europe PMC Funders Author Manuscripts

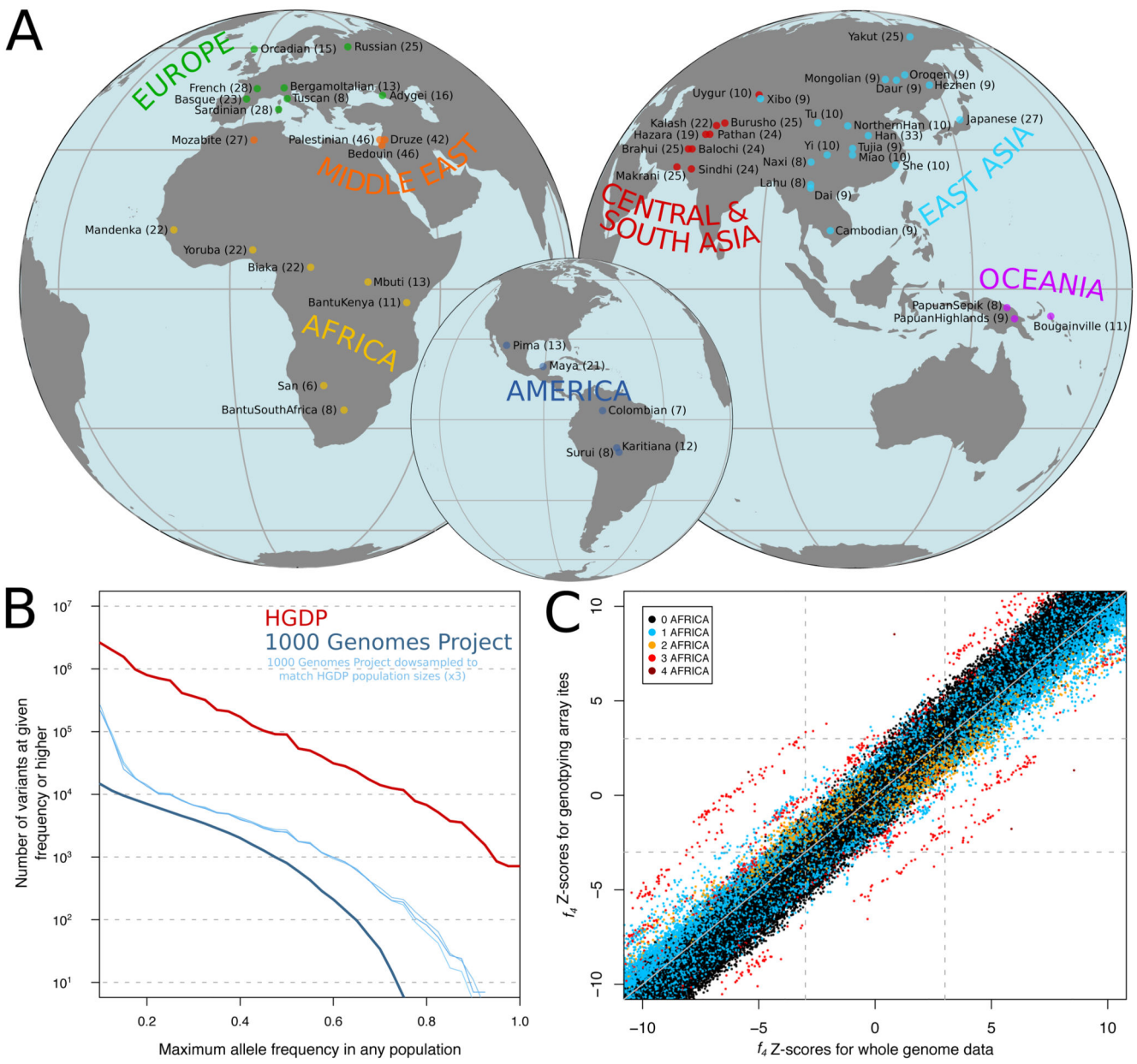

Figure 1. Genome sequencing and variant discovery in 54 diverse human populations.

(A) Geographical origins of the 54 populations from the HGDP-CEPH panel, with the number of sequenced individuals from each in parentheses. (B) Maximum allele frequencies of variants discovered in the HGDP dataset but not in the 1000 Genomes phase 3 dataset, and vice versa. The vertical axis displays the number of variants that have a maximum allele frequency in any single population equal to or higher than the corresponding value on the horizontal axis. To account for higher sampling noise due to smaller population sample sizes in the HGDP dataset, results obtained on versions of the 1000 Genomes dataset down-sampled to match the HGDP sizes are also shown. To conservatively avoid counting variants that are actually present in both datasets but not called in one of them for technical reasons, any variant with a global frequency of >30% in a dataset is excluded. (C) Comparison of Z-

scores from all possible f_4-statistics involving the 54 populations using whole genome sequences and commonly used, ascertained genotyping array sites (8). Points are coloured according to the number of African populations included in the statistic.

Europe PMC Funders Author Manuscripts

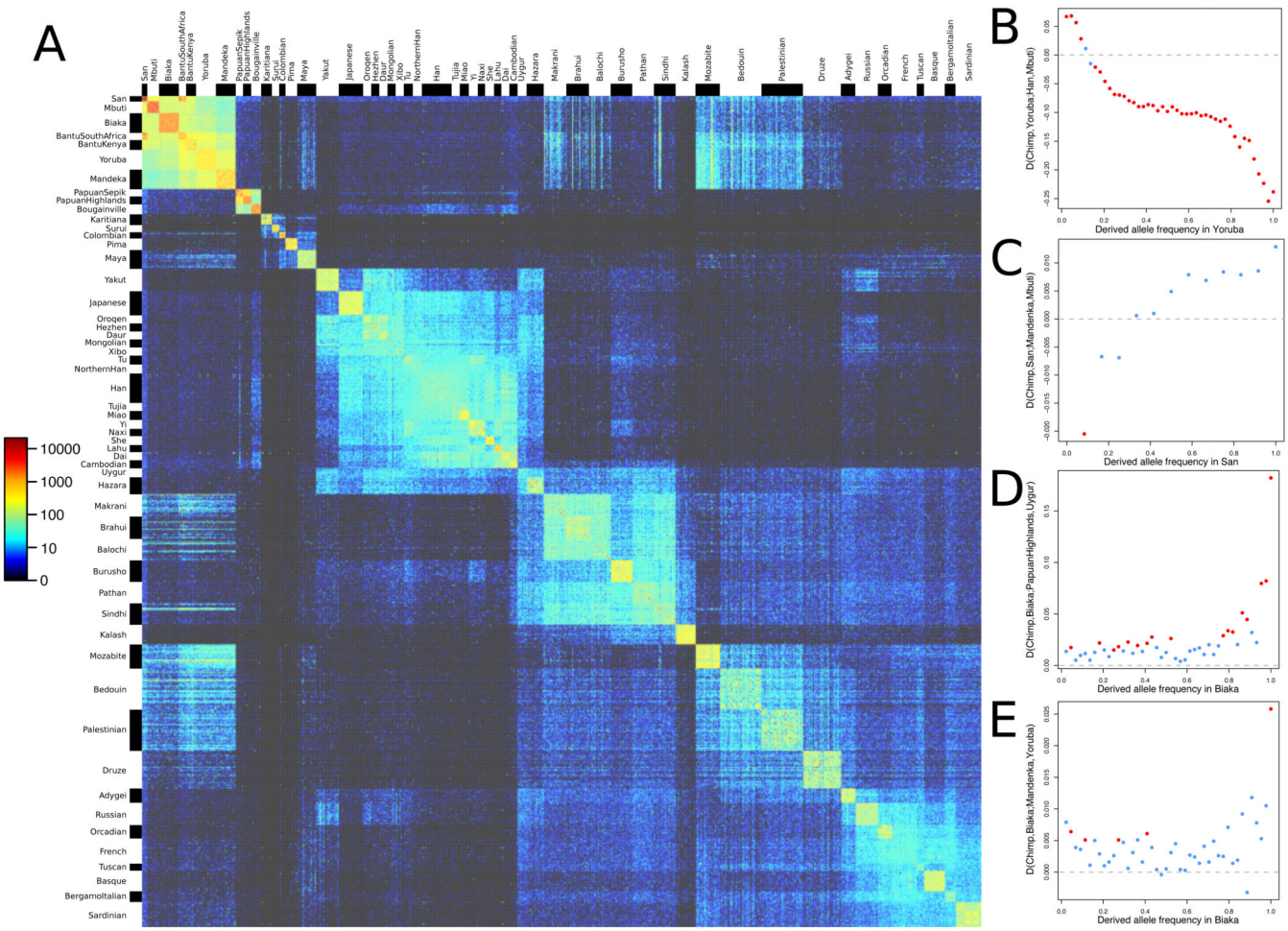

Figure 2. Insights into population relationships from low-frequency variants.

(A) A heatmap of pairwise counts of doubleton alleles (alleles observed exactly twice across the dataset) between all 929 individuals, grouped by population. (B-D) *D*-statistics of the form *D(Chimp,X;A,B)*, stratified by the derived allele frequency in X. Red points correspond to |Z| > 3.

Europe PMC Funders Author Manuscripts

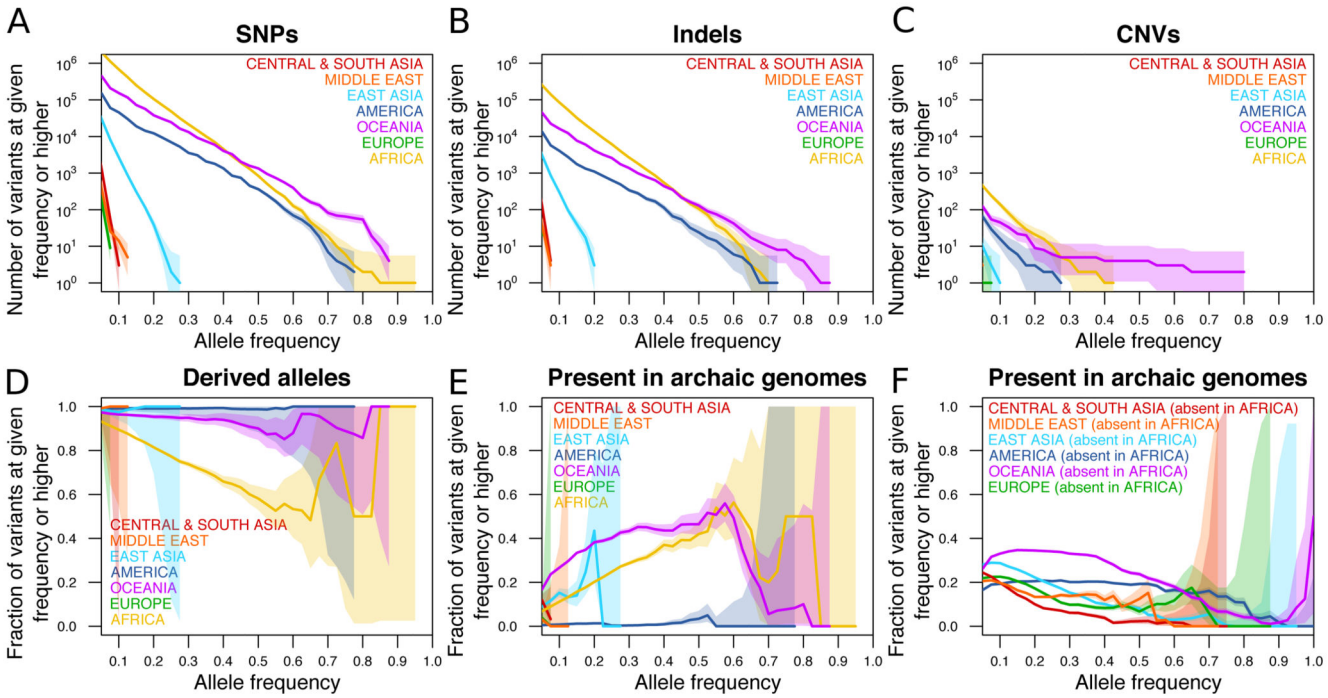

Figure 3. Counts and properties of geographically private variants.

(A-C) Counts of region-specific variants. The vertical axis displays the number of variants private to a given geographical region that have an allele frequency in that region equal to or higher than the corresponding value on the horizontal axis. Shaded areas denote 95% Poisson confidence intervals. (A) SNPs. (B) Indels. (C) CNVs. (D) The fraction of SNPs private to a given region and at a frequency equal to or higher than the corresponding value on the horizontal axis for which the private allele is the derived as opposed to ancestral state. (E) The fraction of SNPs private to a given region and at a frequency equal to or higher than the corresponding value on the horizontal axis for which the private allele is observed in any of three high-coverage archaic genomes. (F) As E, but now counting variants that are present in the given region and absent in Africa, regardless of their frequency elsewhere.

Europe PMC Funders Author Manuscripts

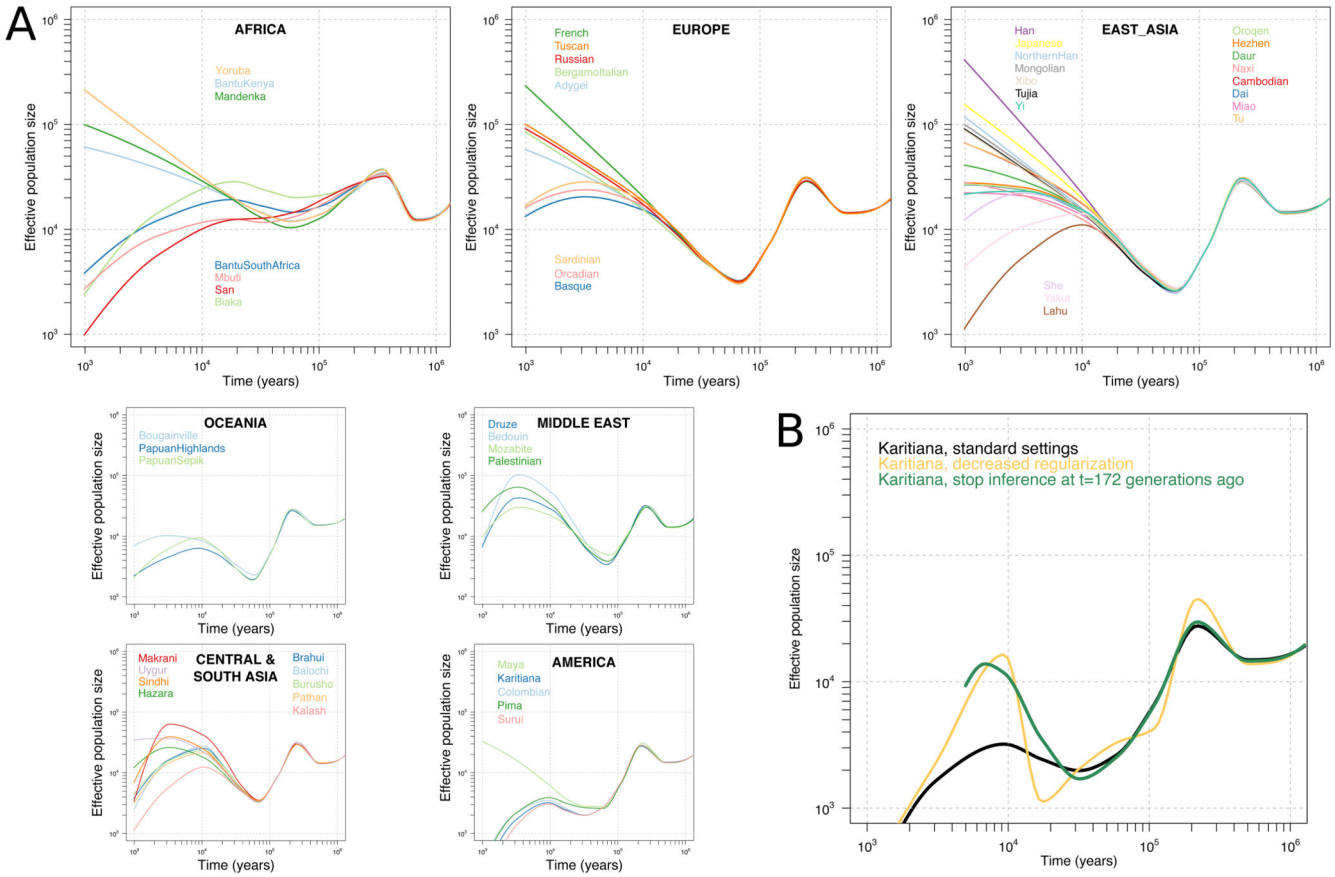

Figure 4. Effective population size histories of 54 diverse populations.

(A) Effective population sizes for all populations inferred using SMC++, computed using composite likelihoods across six different distinguished individuals per population. Our ability to infer recent size histories in some South Asian and Middle Eastern populations might be confounded by the effects of recent endogamy. (B) Results for the Native American Karitiana population with varying SMC++ parameter settings. Decreasing the regularization or excluding the last few thousand years from the time period of inference leads to curves displaying massive growth approximately in the period 10 to 20 kya.

Europe PMC Funders Author Manuscripts

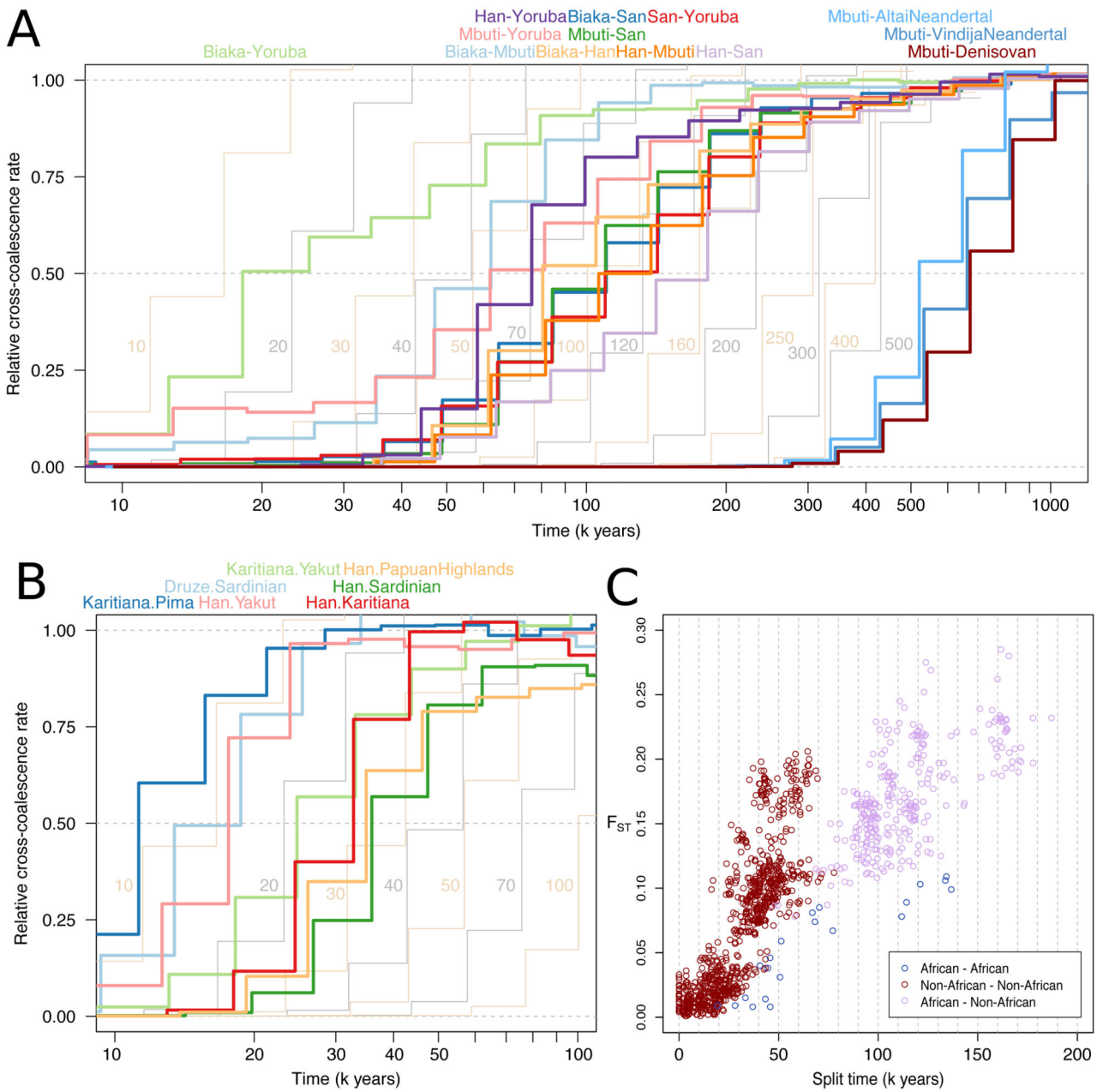

Figure 5. The time depth and mode of population separations.

(A) MSMC2 cross-population results for pairs of African populations, including Han Chinese as a representative of non-Africans, as well as between archaic populations and Mbuti as a representative of modern humans. Curves between modern human groups were computed using four physically phased haplotypes per population, while curves between modern and archaic groups were computed using two haplotypes per population and unphased archaic genomes. The results of simulated histories with instantaneous separations at different time points are displayed in the background in alternating yellow and grey curves. (B) MSMC2 cross-population results, as in A, for pairs of non-African populations. (C) Split times estimated under simple, sudden pairwise split models using momi2 for all

Europe PMC Funders Author Manuscripts

possible pairs among the 54 populations against F_{ST}, a measure of allele frequency differentiation. The plot does not include Native American populations, as we could not obtain reliable momi2 fits for these.

Europe PMC Funders Author Manuscripts

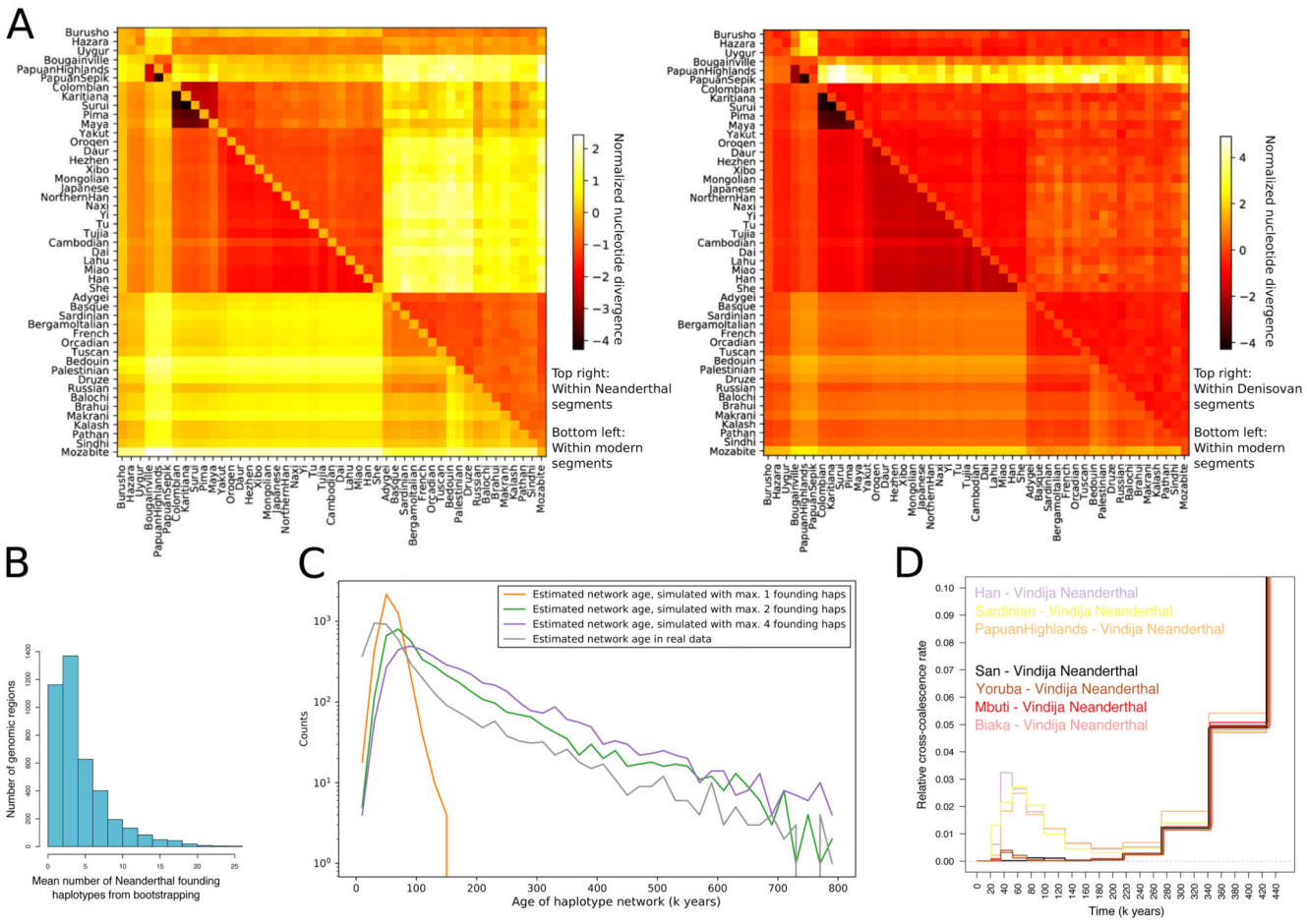

Figure 6. Archaic haplotypes in modern human populations.

(A) Nucleotide divergence D_{XY} within segments deriving from archaic admixture and within other segments in non-African populations. (B) The mean number of archaic founding haplotypes estimated by constructing maximum likelihood trees for each archaic segment identified in present-day non-Africans, and then determining the number of ancestral branches in the tree at the approximate time of admixture (2000 generations ago). (C) The distribution of estimated ages of archaic haplotype networks in the present-day human population. The distribution is compared to results obtained in simulations performed with different numbers of archaic founding haplotypes. (D) MSMC2 cross-population results for African (two individual curves per population) and selected non-African (one individual curve per population) against the Vindija Neanderthal, zooming in on the signal of Neanderthal genome flow in modern human genomes (note the highly reduced range of the vertical axis).

Europe PMC Funders Author Manuscripts